ELSEVIER

Diamond and Related Materials 8 (1999) 657–662

DIAMOND AND RELATED MATERIALS

Confocal Raman imaging for the analysis of CVD diamond films

A. Haouni [a,b], M. Mermoux [a,*], B. Marcus [a], L. Abello [a], G. Lucazeau [a]

[a] *Laboratoire d'Electrochimie et de Physicochimie des Matériaux et Interfaces, UMR 5631 INPG-CNRS, associée à l'UJF, Domaine Universitaire, BP 75, 38402 Saint Martin d'Hères, Cedex, France*

[b] *Université Chouaib Doukkali, faculté des Sciences, B.P. 20, El Jadida, Morocco*

Received 22 July 1998; accepted 16 September 1998

Abstract

Raman imaging has been used to investigate the microstructure of some (100)-textured diamond films. Results have shown that different crystals within a film can give rise to different Raman line positions, intensities and line widths, with the result that the overall diamond line is the sum of all the individual contributions from all the different crystals. The images presented herein first show considerable variation in the distribution of amorphous carbon and defects producing the luminescence background. These defects were mostly detected within the grain boundaries, confirming most of the previous studies. These examples also emphasize the amount of variability that may be detected in the line shape of the Raman diamond line. In particular, line splitting was observed for all the samples examined, and in some particular cases was the most dominant feature that was observed. Such a line splitting has to be related to strain fields that exist within the crystals. However, it was impossible to correlate line shift or line splitting to the presence of defects such as amorphous carbon or point defects giving rise to the luminescence background.

Keywords: Confocal Raman spectroscopy; Defects; Diamond films; Strain

1. Introduction

The growth of chemical vapour deposition (CVD) diamond films is known to be accompanied by the incorporation of non-diamond phases and crystallographic defects, and by the production of stress. Stress in CVD diamond films can lead to film deformation, delamination or even film cracking, while defects limit the normally exceptional functional properties of diamond. Thus, defect detection and measurements of residual stress are necessary to assess the film reliability, and to optimize the deposition process.

The total residual stress in the film is a superposition of thermal stress and intrinsic stress. The former is generated during postgrowth cooling from deposition temperature because of the thermal expansion mismatch of diamond and substrate material. The intrinsic stress is thought to arise mainly from impurities and defects such as grain boundaries, twins, dislocations, amorphous carbon and voids incorporated during diamond growth [1–3]. A number of studies have shown that the intrinsic stress is a complex function of the growth conditions [1,4–7]. Furthermore, it is known from in situ Raman studies that the average intrinsic stress level within the film is thickness dependent [8]. Thus, any information on stress magnitude and on its spatial distribution, may be useful for understanding the growth mechanism itself and assist in the search for methods of improving diamond quality.

There have been numerous studies using Raman spectroscopy to measure stress in CVD diamond films. These studies have shown that different crystals within a film can give rise to different Raman line positions, intensities and line widths and sometimes to a splitting of the diamond peak into two or even three components [9–13]. These shifts are usually interpreted in terms of stresses within the crystals or the films and, in the case of shift and splitting, in terms of anisotropic stresses which distort the cubic symmetry of the diamond lattice, resulting in lifting the triple degeneracy of the Raman diamond peak. The effect of stress on the diamond line shape and position has been theorically described in a number of papers and it is shown that the stress dependence of both the shift and splitting of the peak varies with crystallographic orientation [2,14–16].

* Corresponding author. Fax: 0033 4 76 82 66 77;
e-mail: michel.mermoux@lepmi.inpg.fr

0925-9635/99/$ – see front matter
PII: S0925-9635(98)00253-2

To get a picture of stress distribution, and to try to establish correlations between stress and defects incorporation, we used the possibilities offered by Raman imaging techniques which were earlier described in a number of papers [12–18]. In this work, the surface of two different (100)-textured films grown either on a silicon substrate or a cemented tungsten carbide substrate were mapped at high spatial resolution. The origin of the multiple Raman peaks observed in continuous CVD diamond films is investigated and the presence of very high local stresses is confirmed.

2. Experimental

Two different samples will be examined in this work. Both were grown using a standard microwave plasma quartz tube reactor. The process conditions were: 400 W microwave power, feed gas: 2% CH_4 in 100 sccm H_2 at 10 Torr, substrate temperature $\sim$750 °C. These process conditions ensured the growth of (100)-textured films. The first sample was grown on a diamond-abraded silicon substrate. Its thickness was 30 μm. The second one was grown on a WC-Co (6 wt% Co) substrate. Its thickness was 120 μm. Prior to deposition, the substrate was treated in HCl in order to etch the cobalt at the surface of the sample.

The Raman spectra were recorded on a DILOR XY confocal Raman spectrometer equipped with a charge-coupled device (CCD) array detector, using the 514.5 nm line of an Ar ion laser. The laser power was held constant through the experiments, with generally 10 mW incident on the sample. A confocal aperture of 600 μm was used, so that the sampling volume was a cylinder of approximate dimensions 0.7 μm in diameter and 4 μm in thickness.

To record the Raman images, the laser spot is moved in a line by means of a mirror scanner. The Raman scatter of the scanning illuminated laser spot is collected in the 180° backscatter configuration and travels along the optical axis through the confocal pinhole. A second mirror scanner is used in phase with the first scanner to distribute the collected light along a line on the entrance slit of the spectrograph. Hence, the Raman scatter originating from the line probed by the scanning laser is imaged as a line on the spectrograph and energy dispersed. The two dimensions of the CCD are used to collect spectral and spatial information of the scanned line simultaneously. The sample under the line-scanning laser spot is subsequently displaced in small increments perpendicular to the direction of the laser scanning until the desired area is mapped to its full extend.

For each of the films considered here, maps of the surface were recorded with a point spacing of 0.5 or 1 μm. Raman images are constructed by computer with the information contained in the spectra (integrated intensities of the lines, frequencies and widths of the lines, background intensity,…). While no explicit polarization analysis was performed, no analyser was placed in front of the entrance slit. However, for diamond crystals oriented in the [100] direction, the intensity of the Raman line in backscattering geometry is a strong function of the angle the E vector of the incident laser beam makes with the [100] direction in the plane of the crystal. Because the Ar ion laser is linearly polarized and the diffraction gratings used in the spectrometer have a strong polarization dependence, strong intensity variations were observed analysing (100)-textured films, depending on the orientation of the crystals with respect to the polarization of the incoming beam. To overcome this effect of crystallite orientation, a polarization scrambler was placed in the exit beam.

Under these experimental conditions, maps consisting of around 1200–4500 individual spectra are obtained within 3–15 h, depending on size, spatial resolution, spectral resolution and the signal to noise ratio required. Generally, the spectra were curve-fitted using mixed Gaussian–Lorentzian line shapes.

3. Results and discussion

The first film under investigation was an example of "moderate" quality diamond film. It contained a number of crystallites with a (100) growth orientation that have flattened off during growth to give square facets. Fig. 1 is a scanning electron micrograph of the film from which the investigation was conducted, Fig. 2 the macro Raman spectrum which was obtained by averaging the 4480 spectra used to generate the images presented below. The full width at half maximum of the diamond line is quite low (3.3 cm^{-1}), and the average frequency

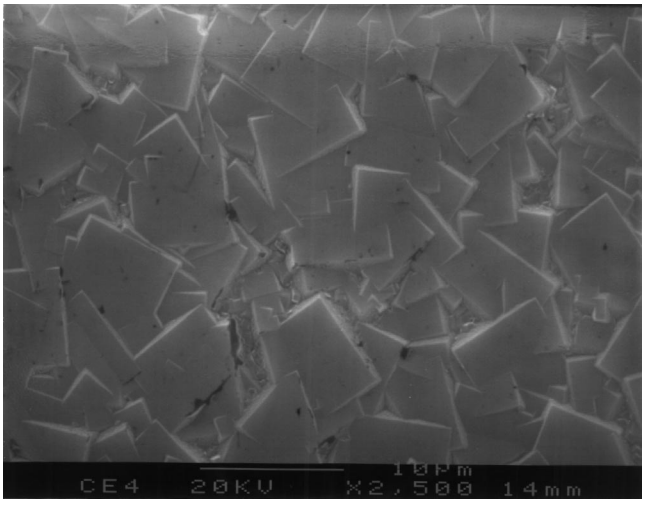

Fig. 1. A scanning electron micrograph of the first sample.

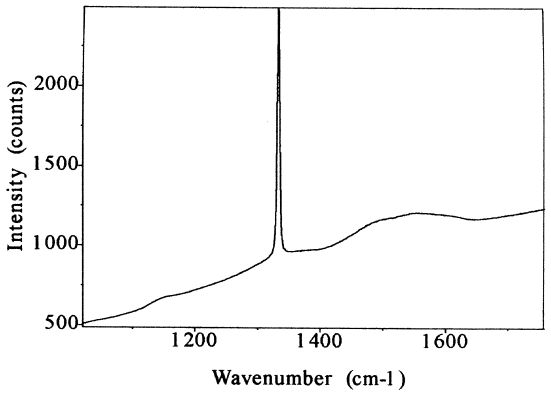

Fig. 2. Macro-Raman spectrum of the first sample, obtained by averaging the 4480 spectra used to generate the images presented in Fig. 3.

(1332.9 cm^{-1}) indicates that the film is under a slight compressive stress. Amorphous carbon is also detected along with a strong luminescence background.

Different maps of the surface, recorded with a point spacing of 0.5 μm, were generated from the spectra: intensity of the diamond line; background intensity; intensity of the amorphous carbon bands; frequency and width of the diamond line. These maps are shown in Fig. 3, along with the optical image of the area of interest. From this figure, it is first noticed that the map of the intensity of the diamond line correlates well with the optical image: it is possible to identify all the individual crystallites. The maps also show that the (100) growth sectors do contain some defective material: amorphous carbon evidenced by a broad band in the Raman spectra peaking near 1500 cm^{-1}, and certain luminescence features usually associated with defects in diamond, giving rise to broad bands superimposed on the Raman spectra. The distribution of this defective material within the surface of the film is not homogeneous. The amorphous carbon and the intensity of this luminescence background illustrated by the lightest shadings mostly lies within the grain boundaries. Moreover, the two maps correlates well with each other, suggesting that these defects are located within the same regions of the film, mainly within the grain boundaries. The similarity of these two images was a very reproducible feature and was found for all the samples analysed. Generally, within these defective regions of the film, the intensity of the diamond line is lower than that arising from defect-free regions, suggesting that this loss in intensity is mostly related to local variations in the

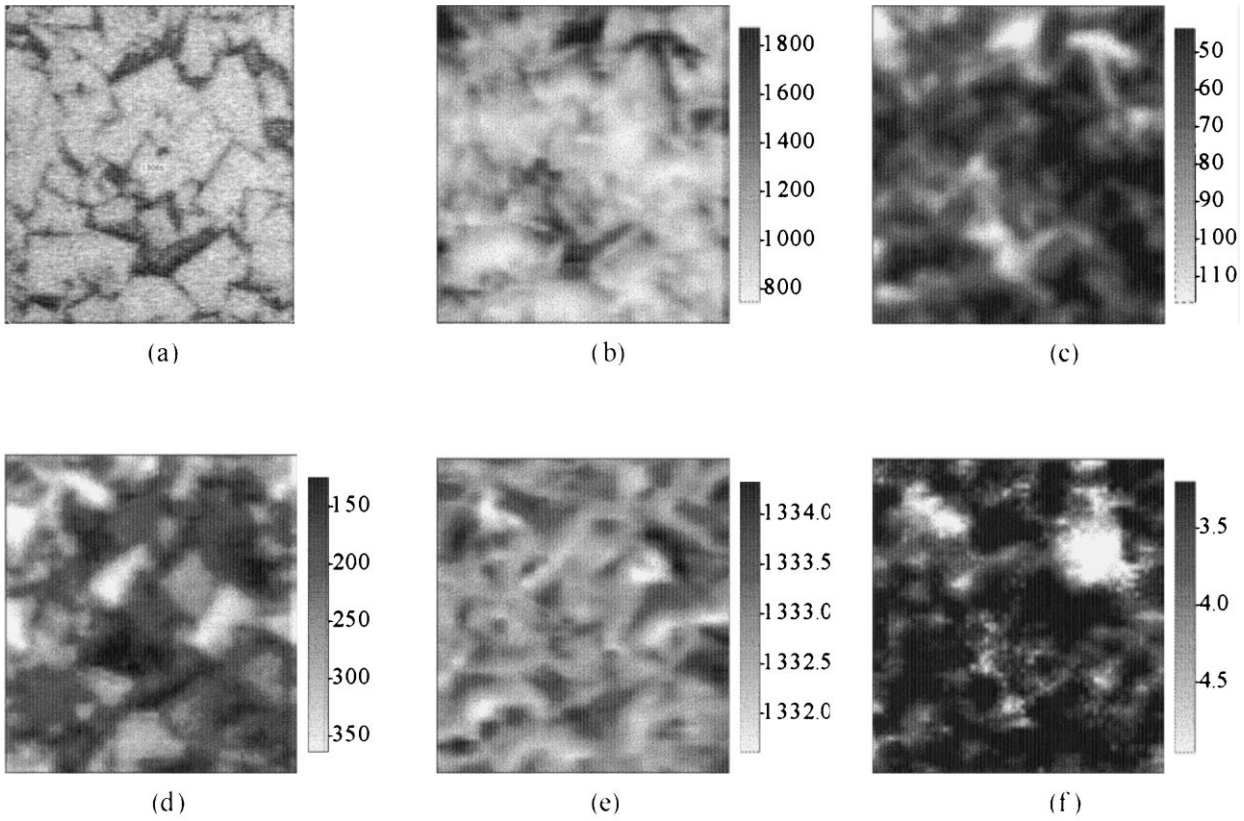

Fig. 3. Raman maps of the background intensity measured at 1650 cm^{-1} (b), the integrated intensity of the amorphous carbon signal (c), the integrated intensity of the diamond line (d), the frequency of the diamond line (e) and the full-width at half maximum of the diamond line (f). (a) Optical image of the area which was examined (30 × 35 μm). Frequency and width of the diamond line were obtained by fitting all the individual spectra.

absorption coefficient. However, loss of intensity of the diamond line may be related to other causes, in particular differences of focusing induced by the roughness of the film, and will be not further discussed within this paper.

For ca 90% of the spectra, the diamond line was symmetrical, and has been curve-fitted using mixed Gaussian–Lorentzian line shapes. The position of the diamond line varied across the sample, although the variations were in general low: $\pm 1\,cm^{-1}$ from the position measured for natural diamond ($1332.5\,cm^{-1}$). Nevertheless, it was possible to detect regions for which the diamond line was found downshifted or upshifted to as high as $2\,cm^{-1}$. These regions are represented in Fig. 3e. These regions are randomly distributed within the film, and in particular do not correspond to grain boundaries. Other measurements not presented here have confirmed this observation. In the same way, the width of the diamond line was in general found in the $2.5–4.5\,cm^{-1}$ range. There is also a large variation evident, even between points separated by as little as 1 μm. In more rare cases, the diamond line exhibited a higher broadening. Within these regions of a few micrometres in diameter (displayed in Fig. 3f), the line was not symmetrical, and large variations in the diamond line shape were observed there. Two significant peaks were needed to fit the data. Examples of such spectra are presented in Fig. 4.

The second film under investigation is an example of highly stressed diamond film. Its morphology is quite similar to that of the first film presented here, but the (100) facets are slightly larger (up to 10 μm). The macro Raman spectrum, obtained as previously described, is presented in Fig. 5. The full width at half maximum of the diamond line is larger ($6.3\,cm^{-1}$), and the average frequency ($1334\,cm^{-1}$) indicates that the film is under high compressive stress. This high compressive stress is mostly related to the difference in the thermal expansion coefficients of the substrate and the film. Moreover, depth resolved measurements have shown that this average frequency is thickness dependent: 30 μm below the surface, the average frequency was found to be near to $1337\,cm^{-1}$.

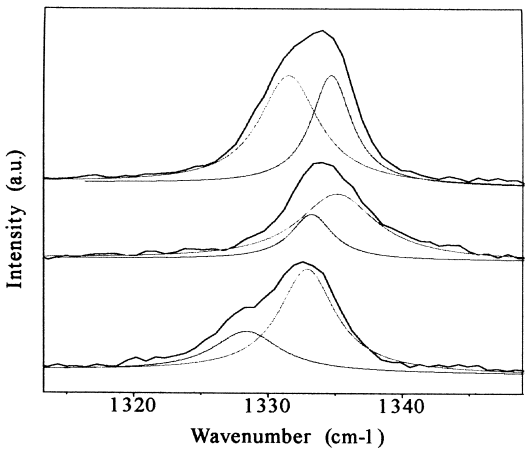

Fig. 4. Examples of spectra extracted from the Fig. 3f.

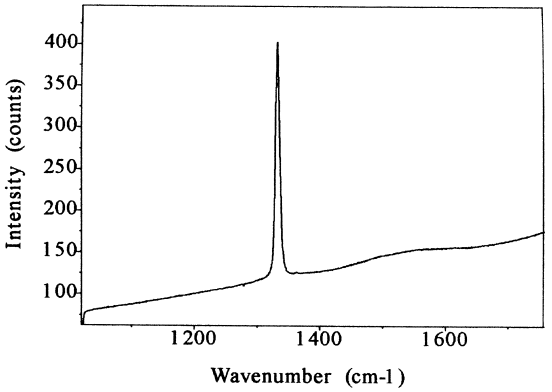

Fig. 5. Macro-Raman spectrum of the second sample, obtained by averaging the 1200 spectra used to generate the images presented in Fig. 6.

The maps presented in Fig. 6 were recorded with a point spacing of 1 μm. The overall qualitative observations are similar to those reported for the first sample: the amorphous carbon and the luminescent defects are mainly located within the grain boundaries, and there are large variations in the frequency and the width of the diamond line. However, higher variations in the frequency and the width of the diamond line were detected. In particular, the frequency was found to evolve in the 1328.5–1338.5 wavenumber range (approximately $\pm 5\,cm^{-1}$ from the average frequency), and most of the spectra displayed an asymmetric line shape. In order to get a better description of the diamond line shape, the same area was examined using the high dispersion mode of the spectrometer. Examples of spectra are presented in Fig. 7 to give an idea of the different situations encountered. In some cases, a single narrow line is observed (upper trace in Fig. 7) and this could correspond to a near perfect region. However, the frequency of this line was found to evolve in a large wavenumber range, suggesting a near hydrostatic stress state, either tensile or compressive. But the most common situation was that where several components are observed. For instance, three components were observed at 1324.5, 1329.3 and $1339.5\,cm^{-1}$ (lower trace in Fig. 7) corresponding to the centre of an apparently well defined crystal. Other situations were detected for which two lines were needed to fit the experimental data, the first downshifted and the second upshifted from the position measured for natural diamond. In most cases and with the exception of spectra recorded near the grain boundaries, the width of the individual components remains as low as $2–4\,cm^{-1}$. However, a

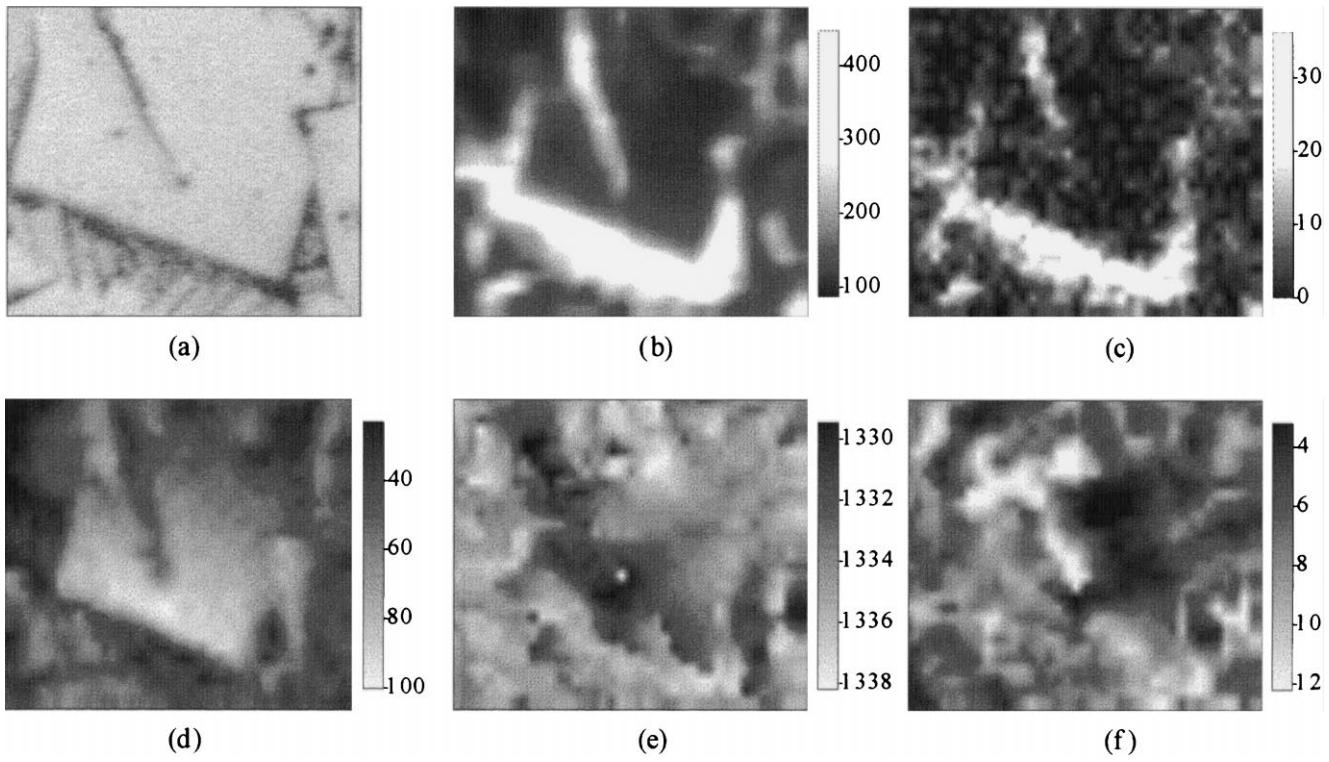

Fig. 6. Raman mapping of the second sample. Raman maps of the background intensity (b), the integrated intensity of the amorphous carbon signal (c), the integrated intensity of the diamond line (d), the frequency of the diamond line (e) and the full-width at half maximum of the diamond line (f). (a) Optical image of the area which was examined (30×40 μm).

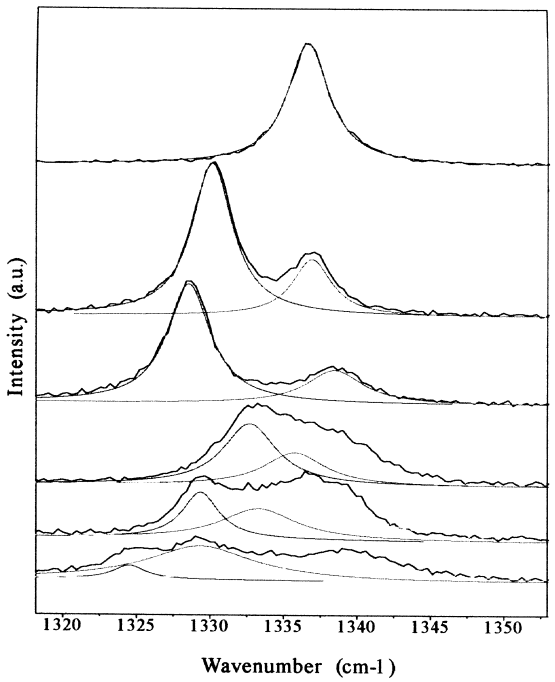

Fig. 7. Examples of high resolution spectra extracted from the images presented in Fig. 6.

high broadening of the lines is seen near the grain boundaries.

Within the two different cases presented here, it is not possible to correlate stress formation and defects such as presence of amorphous carbon, grain boundaries or point defects giving rise to the luminescence background. Thus, it seems that these results have to be associated to highly heterogeneous strain fields occurring over micron dimensions, most probably associated with the more dominant planar structural defects observed in diamond, twins, stacking faults and dislocations. Similar observations have been obtained for the analysis of defective high temperature–high pressure synthetic diamond crystals, for which no non-diamond phases have been detected. Similar observations are also reported in Refs [12,13] concerning either the study of isolated crystals or continuous films.

In principle, the magnitude of the splitting (frequency difference of the two peaks) of the diamond line may be considered as a measure of stress. However, these double peaks rarely satisfy the correlation between absolute peak shift and splitting required by theory. In particular, several spectra are found to exhibit diamond signals composed of two elementary peaks, the first one downshifted and the second upshifted from the position measured for natural diamond (fourth and fifth spectra in Fig. 7). Thus, there are small regions of high tensile stress which coexist with regions of high compressive stress, as if different regions within the film constrain each other. Thus, it may be thought that the diamond line profile reflects a local mechanical equilibrium.

4. Conclusion

Confocal micro-Raman spectroscopy, when used with appropriate mapping stages, is an efficient quality control tool. Raman mapping produces high spectral resolution data that can be used to investigate samples over micrometer distance scales. The images presented herein first show considerable variation in the distribution of amorphous carbon and defects producing the luminescence background. These defects were mostly detected within the grain boundaries, confirming most of the previous studies. The examples presented herein also emphasize the amount of variability that may be detected in the line shape of the Raman diamond line. In particular, line splitting was more or less observed for all the samples examined, and in some particular cases is the most dominant feature that was observed. Such a line splitting has to be related to strain fields that exist within the crystals. However, it was impossible to correlate line shift or line splitting to the presence of defects such as amorphous carbon or point defects giving rise to the luminescence background. Thus, it seems that these highly heterogeneous strain fields which are observed over micron dimensions have to be associated with the more dominant planar structural defects observed in diamond, namely twins, stacking faults and dislocations. It is worth noting that all these information are missing examining more usual macro-Raman spectra, which are in general very reproducible over the samples.

References

[1] H. Windischmann, G.F. Epps, Y. Cong, R.W. Collins, J. Appl. Phys. 69 (1991) 2231.
[2] Y. Von Kaenel, J. Stiegler, J. Michler, E. Blank, J. Appl. Phys. 81 (1997) 1726.
[3] L. Bergman, R. Nemanich, J. Appl. Phys. 78 (1995) 6709.
[4] S.J. Harris, A.M. Weiner, S. Prawer, K.W. Nugent, J. Appl. Phys. 80 (1996) 2187.
[5] H. Guo, M. Alam, Thin Solid Films 212 (1992) 173.
[6] J.A. Baglio, B.C. Farnsworth, S. Hankin, G. Hamill, D. O'Neil, Thin Solids Films 212 (1992) 180.
[7] M.S. Haque, H.A. Naseem, A.P. Malshe, W.D. Brown, Chem. Vap. Deposition 3 (1997) 129.
[8] M. Mermoux, L. Fayette, B. Marcus, N. Rosman, L. Abello, G. Lucazeau, Analysis 23 (1995) 325.
[9] L. Fayette, M. Mermoux, B. Marcus, F. Brunet, P. Germi, M. Pernet, L. Abello, G. Lucazeau, J. Garden, Diamond Relat. Mater. 4 (1995) 1243.
[10] S.A. Stuart, S. Prawer, P.S. Weiser, Appl. Phys. Lett. 62 (1993) 1227.
[11] S.A. Stuart, S. Prawer, P.S. Weiser, Diamond Relat. Mater. 2 (1993) 753.
[12] K.W. Nugent, S. Prawer, Diamond Relat. Mater. 7 (1998) 215.
[13] I.I. Vlasov, V.G. Ralchenko, E.D. Obraztsova, A.A. Smolin, V.I. Konov, Appl. Phys. Lett. 71 (1997) 1789.
[14] E. Anastassakis, A. Pinczuk, E. Burstein, F.H. Pollak, M. Cardona, Solid State Commun. 8 (1970) 133.
[15] M.H. Grimdistch, E. Anastassakis, M. Cardona, Phys. Rev. B 18 (1978) 901.
[16] J.W. Ager III, M.D. Drory, Phys. Rev. B 48 (1993) 2601.
[17] I.P. Hayward, K.J. Baldwin, D.M. Hunter, D.N. Batchelder, G.D. Pitt, Diamond Relat. Mater. 4 (1995) 617.
[18] C.D.O. Pickard, T.J. Davis, W.N. Wang, J.W. Steeds, Diamond Relat. Mater. 7 (1998) 238.